Fourier transform infrared spectroscopy characterization of the lamellar and nonlamellar structures of free lipid A and Re lipopolysaccharides from *Salmonella minnesota* and *Escherichia coli*

Klaus Brandenburg
Forschungsinstitut Borstel, D-2061 Borstel, Germany

ABSTRACT The structural polymorphism of free lipid A and deep rough mutant lipopolysaccharide (LPS Re) from *Salmonella minnesota* strain R595 and *Escherichia coli* strain F515 was characterized by Fourier transform infrared (IR) spectroscopy. For this, the $\beta \leftrightarrow \alpha$ phase states and the three-dimensional supramolecular structures, the latter deduced from small-angle synchrotron radiation x-ray diffraction, were investigated at different water contents, Mg^{2+} concentrations, and temperatures. The analysis of the IR data for vibrations originating from the hydrophobic moiety shows that the $\beta \leftrightarrow \alpha$ acyl chain melting is strongly expressed only for the stretching and scissoring modes of the methylene groups. Vibrational groups originating from the interface region sense the acyl chain melting well (ester carbonyl bands) or only weakly (amide bands), and those resulting from the pure polar moiety not at all. From the x-ray data, the existence of lamellar (L), different cubic, and, for lipid A and LPS R595, also inverted hexagonal (H_{II}) structures could be proven in the temperature range 20–80°C with cubic $\leftrightarrow$ cubic and cubic $\leftrightarrow H_{II}$ transitions for the Mg^{2+}-free and $L \leftrightarrow H_{II}$ transitions for the Mg^{2+}-containing samples. These structural transitions can be characterized most readily by specific changes of the vibrational bands resulting from the interface region: the ester carbonyl and the amide bands. The magnitude of the changes corresponds to that of the structural rearrangement, i.e., is highest for the $L \leftrightarrow H_{II}$, lower for the cubic $\leftrightarrow H_{II}$, and lowest for the cubic $\leftrightarrow$ cubic transitions. The structural transitions are only marginally expressed for vibrational bands of the hydrophobic moiety. Similarly, the band contours of vibrations from the hydrophilic region are no indicators of the structural reorientations except for the carboxylate bands of LPS Re. Particularly the stretching vibrations of the phosphate groups are nearly completely invariant; the absolute values of their half bandwidths, however, differ significantly for lipid A and LPS Re, which seems to be of biological relevance.

The ability of IR spectroscopy to detect supramolecular changes also beyond the measureability by x-ray diffraction, i.e., at water contents > 95 to 99.5%, is demonstrated.

INTRODUCTION

Lipopolysaccharides (LPS)[1] are the major amphiphilic constituents of the outer leaflet of the outer membrane of Gram-negative bacteria. They consist of an oligo- or polysaccharide moiety and a covalently linked lipid portion, termed lipid A, anchoring the LPS molecules in the membrane (1). In mammals, LPS induce various biological effects as constituents of the bacterial outer membrane as well as in free form (2, 3) and are, therefore, called the endotoxins of Gram-negative bacteria. The molecular mechanisms triggering the cell response to endotoxic provocation are far from being understood. Independent of the kind of interaction, however, the elucidation of the physicochemical behavior of LPS in aqueous solutions should be important, i.e., of the three-dimensional supramolecular structures of LPS aggregates and within these, the state of order of their hydrocarbon chains. In various previous reports, the $\beta \leftrightarrow \alpha$ gel to liquid crystalline acyl chain melting behavior for endotoxins could, on the whole, be determined unequivocally (4). Enterobacterial LPS exhibit at higher water contents (>90%) an acyl chain melting at a temperature T_c = 30°C for deep rough mutant LPS, whereas free lipid A has a T_c around 45°C (5–7). The values of T_c and the state of order within each phase were found to depend strongly on ambient conditions like water content and salt concentration, e.g., Mg^{2+} (6, 8).

The question of which supramolecular aggregate structures are adopted by LPS and free lipid A was not answered consistently in former publications. For example, for different LPS and lipid A preparations at various water and Mg^{2+} contents, a variety of three-dimensional arrangements were found or postulated (5, 7–12). For clarifying these partially contradictory results, complete phase diagrams were established recently, i.e., in a first step for free lipid A and deep rough mutant LPS from *Salmonella minnesota* and *Escherichia coli* using synchrotron x-ray small-angle diffraction (13–15). From these results and those on LPS with longer sugar chains (Brandenburg, K., unpublished data), it can be stated that despite the high brilliance of synchrotron radiation, an unequivocal structural determination at water contents > 80% is difficult or even impossible, bearing in mind at the same time that in most biological systems the LPS content is lower than 1%. Moreover, because of the restricted availability of synchrotron radiation, it would be most advantageous if other experimental techniques could be applied. In this context, ^{31}P-nuclear magnetic resonance (NMR) has been used successfully for various phospholipid/water systems (16, 17). However, beside similar limitations with respect to measurements at high water content, interpretational difficulties arise

Address correspondence to Dr. Klaus Brandenburg.

[1] *Abbreviations used in this article:* FT, Fourier transform; IR, infrared; LPS, lipopolysaccharide(s); PE, phosphatidylethanolamine.

0006-3495/93/04/1215/17 $2.00

when so-called "isotropic signals" occur, which might correspond, for example, to small unilamellar vesicles but also to structures with cubic symmetry.

Infrared (IR) spectroscopy has been applied successfully for the elucidation of the physical behavior of various phospholipid/water systems, e.g., the characterization of the state of order of their hydrocarbon chains and the changes under the influence of different pH, salt concentrations, and temperatures (18, 19). Furthermore, the detailed analysis of IR-active vibrations resulting from the polar and the apolar moiety, respectively, gave a lot of information on intra- and intermolecular interactions. Attempts to directly correlate three-dimensional conformations to IR data were, however, undertaken by only few authors. In particular, Mantsch et al. (20, 21) investigated temperature-controlled transitions of fully hydrated bacterial and erythrocyte-extracted phosphatidylethanolamine (PE) from the lamellar β to α phase (L_β to L_α) and then into the inverted hexagonal (H_{II}) structure. They found phase- and structure-characteristic changes in the peak position, half widths, and intensity of certain vibrational bands. These investigations, however, were restricted to a small region of the complete phase diagram and could therefore not give general statements about the ability of IR spectroscopy to detect supramolecular structures and transitions between them.

This article is concerned with investigations into the supramolecular structures and phase states of free lipid A and LPS Re from *E. coli* and *S. minnesota*. The structural information from synchrotron x-ray small-angle diffraction is correlated with the specific behavior of IR bands in the polar, interface, and apolar region. The results show that the different lamellar and nonlamellar (cubic, H_{II}) structures of the endotoxins have a particular impact on band position, width, and intensity of some of the investigated vibrations. Whereas the dependence of these parameters on the three-dimensional structures, if at all, is only marginal for the bands originating from the pure hydrophobic and hydrophilic regions, it is well expressed for the vibrations of the interfacial region, particularly for the carbonyl stretching of the ester groups and the amide bands. The results further show that under conditions that are not accessible to the structural elucidation with synchrotron x-ray diffraction (>90–95% water content), a structural determination with IR spectroscopy seems still to be possible.

MATERIALS AND METHODS

LPS and lipid A

As LPS, those from deep rough mutant Re of *E. coli* strain F515 and *S. minnesota* strain R595 were used. The LPS were extracted from bacteria by the phenol/chloroform/light petrol ether method (22), purified and lyophilized, and were taken in their natural or Na^+ salt form. Free lipid A was isolated from LPS Re by acetate buffer treatment, purified, and converted to the triethylamine salt form (23). In Fig. 1, the chemical structure of LPS Re and its hydrophobic moiety lipid A is illustrated. The dashed lines indicate different substitutions of the respective groups in LPS from *E. coli* F515 and *S. minnesota* R595. Furthermore, the locations of the various IR vibrational groups investigated in the present analysis are also shown.

Sample preparation

All LPS and lipid A samples were prepared as aqueous dispersions at different concentrations varying between 50 and 99.5% water content wt/wt. For this, the lyophilized lipids were suspended directly in water or in deuterium oxide or in stock solutions of Mg^{2+} to realize a defined molar [LPS]/[Mg^{2+}] ratio. All lipid samples were temperature cycled at least twice between 4 and 70°C and then stored at 4°C ≥12 h before measurement. Each of the lipid samples was used for the Fourier transform (FT)-IR spectroscopy as well as for the x-ray spectroscopic measurements.

For measurement of IR spectra of anhydrous samples, the endotoxins were suspended in chloroform and an appropriate amount was spread on an attenuated total reflectance ZnSe plate.

X-ray diffraction

X-ray diffraction measurements were kindly performed by Dr. M. H. J. Koch at the European Molecular Biology Laboratory outstation at the synchrotron radiation facility, HASYLAB (C/O DESY, Hamburg, Germany), using the double-focusing monochromator-mirror camera X33 (24). Diffraction patterns in the range of the scattering vector $0.07 < s < 1\ nm^{-1}$ ($s = 2 \cdot \sin\Theta/n \cdot \lambda$, where 2Θ is the scattering angle and λ is the wave-length = 0.15 nm) were recorded with exposure times of 2–3 min using a linear detector with delay line readout (25). The wavelength calibration was done with dry rat tail tendon as a standard having a periodicity of 65 nm. Further details of the data acquisition and evaluation systems can be found elsewhere (26). The measurements were performed in the temperature range from 20 to 80°C, usually in intervals of 10°C. In the diffraction patterns presented here, the logarithm of the diffraction intensities $\log I(s)$ is plotted against the scattering vector s. The evaluation of the x-ray spectra was achieved according to procedures described previously (8, 13–15, 27, 28).

FT-IR spectroscopy

The IR spectroscopic investigations were performed on a FT-IR spectrometer '5-DX' (Nicolet Instruments, Madison, WI). The lipid samples were placed in a CaF_2 or a ZnSe cuvette separated by a thin, 12.5-μm Teflon spacer. Temperature was usually varied automatically between 10 and 85°C with a heating rate of 3°C/5 min. Every 3–4°C, 50 interferograms were accumulated, apodized with a Happ-Genzel function, Fourier transformed, and converted to absorbance spectra. In some cases, subtraction of pure water spectra was performed, which, however, gave no significant improvement of the spectra.

The position of the peak maxima of strong absorption bands can be determined with a precision of better than $0.1\ cm^{-1}$ (11). In the case of weak absorption bands, resolution enhancement techniques, i.e., Fourier self-deconvolution (29–31), were applied after baseline subtraction. In this procedure, three parameters have to be chosen adequately: (*a*) the peak width; (*b*) the resolution enhancement factor, which is a measure of the degree of band narrowing and is usually selected to be highest for a given output signal to noise ratio without producing negative side lobes (30); and (*c*) the bandshape that is composed of a superposition of Gaussian and Lorentzian functions. A factor of 0.3 (Gaussian proportion 70% and Lorentzian 30%) was usually applied, because in this way the deconvoluted spectra were optimally enhanced similar as described in Blume et al. (32). The absorption bands were analyzed with respect to peak position, integrated intensity (peak area), and width. The latter was measured, if possible, at 50% bandheight, i.e., full width at half height, or, in the case of overlapping bands, at a higher bandheight (e.g., 75%). A similar procedure was also applied for the

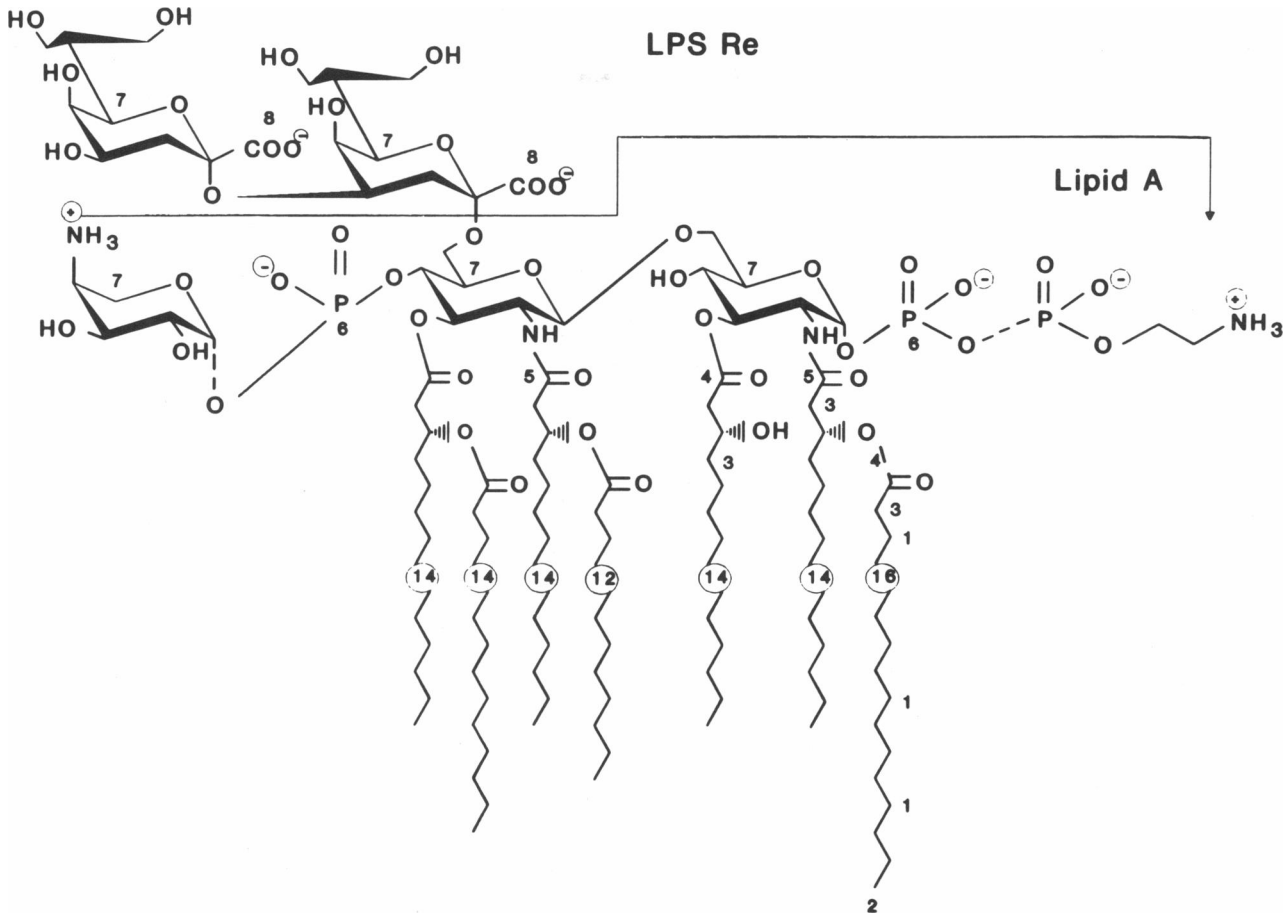

FIGURE 1 Chemical structure of deep rough mutant LPS Re and of free lipid A from *Salmonella minnesota* R595 and *Escherichia coli* F515. The dashed lines within the lipid A moiety indicate incomplete substitution of the respective groups. These should be completely absent in lipid A and LPS Re from *E. coli*.

determination of band intensity. Thus, the absolute values of band intensity and width are not necessarily comparable for the different bands or samples.

The location of the various IR vibrational bands within the lipid A and LPS Re molecules (see band numbering in Fig. 1) and their (tentative) assignment and peak positions (in cm^{-1}) are summarized in Table 1. The assignment was performed according to present knowledge (11, 33–35).

RESULTS

LPS from *S. minnesota* R595

As first and main example, deep rough mutant LPS from *S. minnesota* strain R595 was analyzed with x-ray and IR spectroscopy at a water concentration of 80% in the absence and at an equimolar content of Mg^{2+}, respectively. For a determination of the acyl chain melting behavior, the position of the symmetric stretching of the methylene groups $\nu_s(CH_2)$ is plotted in Fig. 2 for both LPS preparations. Like the antisymmetric stretching mode $\nu_{as}(CH_2)$, this band is a sensitive marker of lipid order or disorder (18). Clearly, the LPS sample in distilled water exhibits a phase transition at $T_c \approx 31°C$ and a transition range between 27 and 35°C, whereas the 1:1 molar sample of LPS and Mg^{2+} has a T_c value of ~40°C with a transition range between 22 and 50°C.

The corresponding x-ray diffraction patterns of the same batches are shown in Fig. 3, *a* and *b*. For the LPS sample without Mg^{2+}, the supramolecular structures can be classified into three distinct temperature ranges: (*a*) between 20 and 45°C, a structure with cubic symmetry occurs (e.g., at 40°C the observed reflections can be indexed to 8.60 nm = $d_Q/\sqrt{3}$, 4.53 nm = $d_Q/\sqrt{11}$, 3.09 nm = $d_Q/\sqrt{24}$, 2.33 nm = $d_Q/\sqrt{42}$, assuming a periodicity d_Q = 15.0 nm) that might belong to space group Q^{224}; between 45 and 65°C, an intermediate nonlamellar structure tentatively termed Q_x is observed; and at $T \geq$ 70°C, the H_{II} structure becomes predominant (d_H = 5.83 nm and 3.42 nm = $d_H/\sqrt{3}$, 2.96 nm = $d_H/\sqrt{4}$). The spectra of the sample [LPS]/[Mg^{2+}] = 1:1 M clearly prove the existence of a pure lamellar phase between 20 and 60°C (occurrence of reflections at equidistant ratios) and a transition into H_{II} at a temperature T_H lying

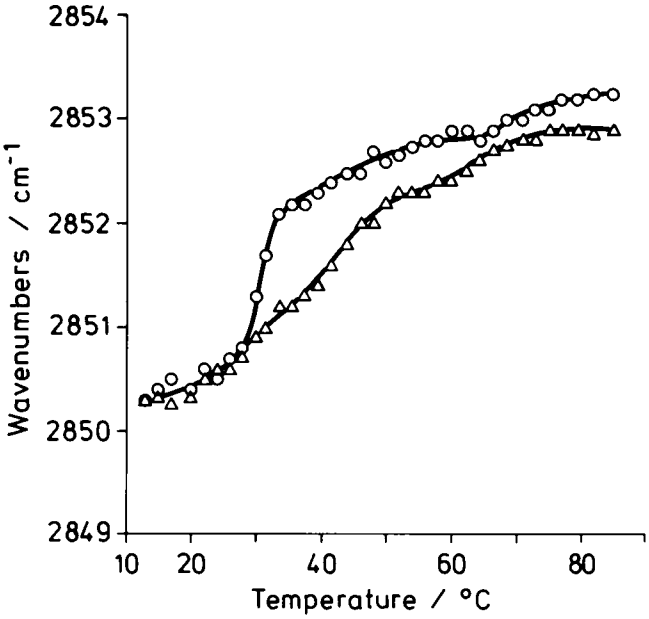

FIGURE 2 Peak position of the symmetric stretching vibration of the methylen groups $\nu_s(CH_2)$ versus temperature for LPS R595 preparations at 80% water content. (○) Without Mg^{2+}; (△) [LPS]/[Mg^{2+}] = 1:1 M.

slightly below 70°C. For further details also at other water and Mg^{2+} contents, see Brandenburg et al. (15).

In Figs. 4, *a* and *b* and 5, *a* and *b*, the corresponding IR spectra, one original and various deconvoluted, are shown in the wavenumber ranges 1,755–1,700 cm^{-1} and 1,580–1,515 cm^{-1}, respectively. On the righthand side of the figures, for the different temperature ranges an assignment to the aggregate structures L, Q, and H_{II} deduced from the x-ray diffraction data according to Fig. 3 is given. The range of the ester carbonyl stretching vibration shows a splitting into three bands lying around 1,743–1,746, 1,727–1,730, and 1,710 cm^{-1} (values are usually given for the lowest temperatures; see Fig. 4, *a* and *b*). The transitions between the nonlamellar structures ($Q_{224} \leftrightarrow Q_x \leftrightarrow H_{II}$) in Fig. 4 *a* for the Mg^{2+}-free sample and the transitions within the lamellar phases (L_β to L_α) and from the lamellar into the H_{II} structure (Fig. 4 *b*) for the Mg^{2+}-containing sample can be differentiated by particular changes of the band contours of the contributing vibrations. For example, the band around 1,710 cm^{-1} broadens when passing from Q_{224} to Q_x and sharpens again when passing into the H_{II} structure (Fig. 4 *a*). A similar situation is found in the range of the amide II vibration, which shows a splitting into three bands at 1,565, 1,550, and 1,533 cm^{-1} (Fig. 5, *a* and *b*). Again, a clear differentiation between the nonlamellar, cubic, and H_{II} (Fig. 5 *a*) on the one hand and lamellar L_β and L_α and H_{II} structures on the other hand (Fig. 5 *b*) is possible.

In the following, the behavior of some of the vibrational bands presented in Figs. 4 and 5 is elucidated in more detail. In Fig. 6 the bandwidths (*a*), intensities (*b*), and peak positions (*c*) of the two main ester vibrational bands at 1,730 and 1,710 cm^{-1} are plotted as functions of temperature for the LPS/water system. The 1,710 cm^{-1}-band seems to be sensitive, but only slightly, to the acyl chain order that is expressed as increase in bandwidth (*a*) and peak position (*c*) and decrease in intensity (*b*). Also, the supramolecular conformations seem to be expressed by an increase in bandwidth and a decrease in band intensity at the Q_{224} to Q_x transition around 50°C (Fig. 6, *a* and *b*) and a drastic increase in band position and intensity and decrease in bandwidth at the transition into H_{II}. The vibration around 1,730 cm^{-1} is a more sensitive indicator of the acyl chain order. This is detectable by the strong increase of bandwidth and position (Fig. 6, *a* and *c*) and decrease of intensity (Fig. 6 *b*). However, for all three parameters, no evidence for the Q_{224} to Q_x transition is found. The transition into the H_{II} structure causes no change in band position, a slight decrease of bandwidth, and a strong increase of band intensity.

The same bands were analyzed in detail also for the Mg^{2+}-containing sample (see Fig. 4 *b*). For example, in Fig. 7, *a* and *b*, the band widths and intensities, respectively, are plotted versus temperature. Some characteristics are found as described for the LPS sample in pure water. The comparison with Fig. 6, *a* and *b* shows, however, that the changes at the $\beta \leftrightarrow \alpha$ acyl chain melting temperature (T_c lying at ~40°C; see Fig. 2) and at the transition into H_{II} are significantly more expressed than for the Mg^{2+}-free sample.

The behavior of the third component in the band contour of the ester carbonyl stretching at ~1,746 cm^{-1} (data not shown) compares well with that at 1,730 cm^{-1}, i.e., the temperature course of the peak position indicates the $\beta \leftrightarrow \alpha$ transition and, only slightly, that into H_{II}. Again, particularly the bandwidth is a sensitive marker of the acyl chain melting and of the transition into H_{II} in that a distinct band broadening at T_c and a narrowing at T_H take place very similarly to the behavior of the 1,730 cm^1-band in Figs. 6 *a* and 7 *a*.

As an example for the temperature dependence of the deconvoluted spectra in the range of the amide II vibration, the intensity of the band at ~1,565 cm^{-1} is plotted for the two LPS samples (Fig. 8). There is no indication for the acyl chain melting. However, the transitions within cubic structures and from cubic to H_{II} for the Mg^{2+}-free sample and from the lamellar to H_{II} for the Mg^{2+}-containing sample are clearly detectable.

In the following, the comprehensive analysis of other IR bands in the wavenumber range 3,500–700 cm^{-1} is described briefly separately for the apolar, interface, and polar region (data not shown).

Vibrations resulting from the apolar moiety

For the bending mode of the end methyl groups $\delta_s(CH_3)$, the band position and width are nearly invariants over the whole temperature range for both LPS prep-

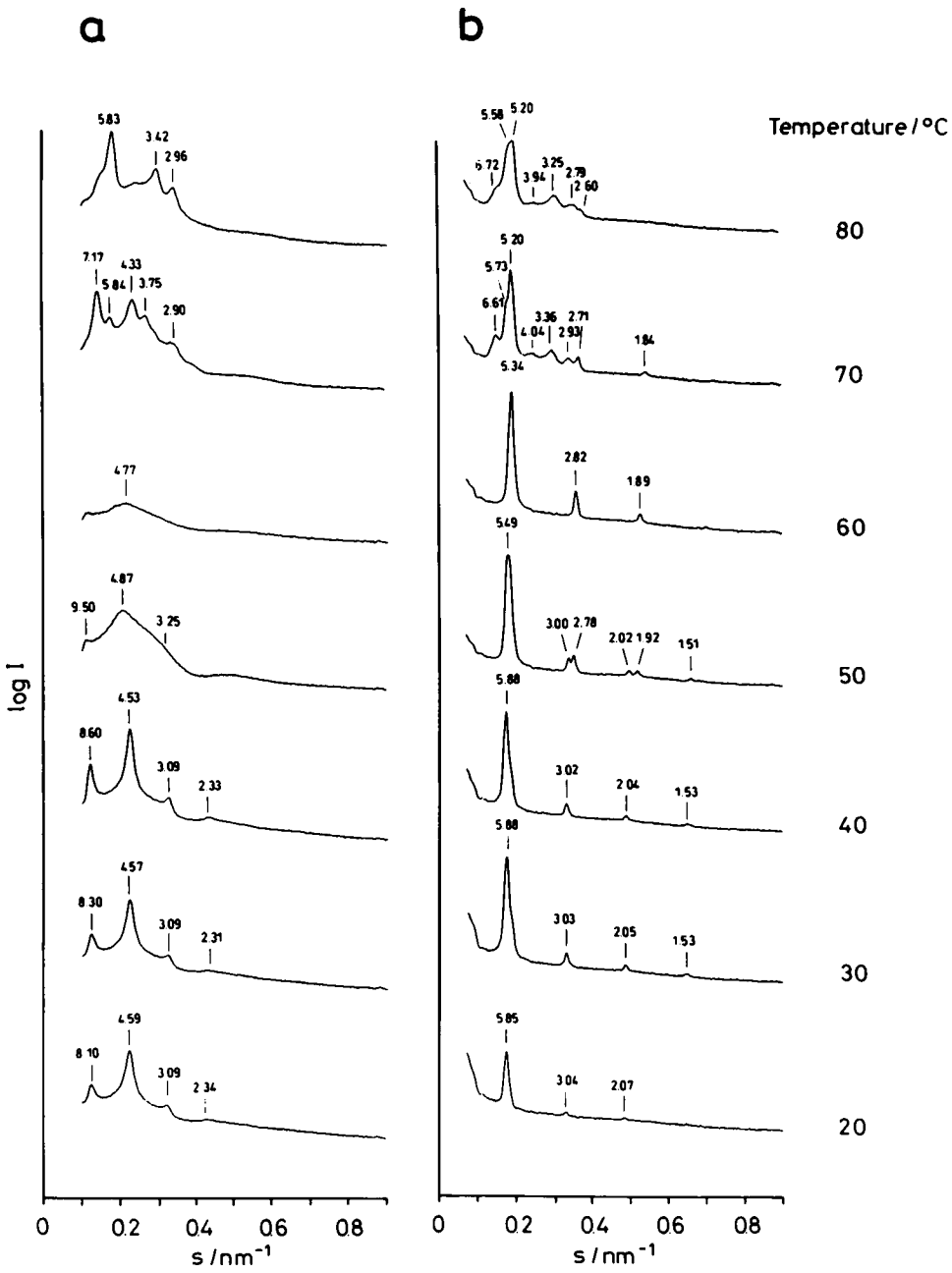

FIGURE 3 Small-angle x-ray diffraction patterns of LPS R595 preparations at 80% water content and at temperatures between 20 and 80°C. (*a*) Without Mg^{2+}; (*b*) [LPS]/[Mg^{2+}] = 1:1 M. The listed spacings are in nm.

arations, whereas the band intensity increases slightly during the $\beta \leftrightarrow \alpha$ transition. The situation for the antisymmetric stretching $\nu_{as}(CH_3)$ is very similar, i.e., nearly no changes take place in band positions and widths and only slight changes of the band intensity at the $\beta \leftrightarrow \alpha$ transition.

The band positions of both components of $\delta(CH_2)$ clearly indicate the acyl chain melting leading to a decrease from ~1,485.5 to 1,484.5 cm^{-1} and from 1,467.5 to 1,466.0 cm^{-1}, respectively, during the gel to the liquid crystalline phase transitions for both LPS preparations. Both bandwidths, however, are nearly invariant at all temperatures. The band intensity decreases considerably at the lamellar to H_{II} transition, whereas a weak decrease is observed for the cubic to H_{II} transition. In contrast, all three band parameters of the main rocking progression band $\gamma_r(CH_2)$ are largely invariant over the whole temperature range.

For the acyl chain modes double-gauche at ~1,353 cm^{-1}, kinks at ~1,366 cm^{-1}, and end-gauche at ≈1,340 cm^{-1} (36, 37), and, furthermore, one band at 1,324 cm^{-1}, which might originate from the single C—H de-

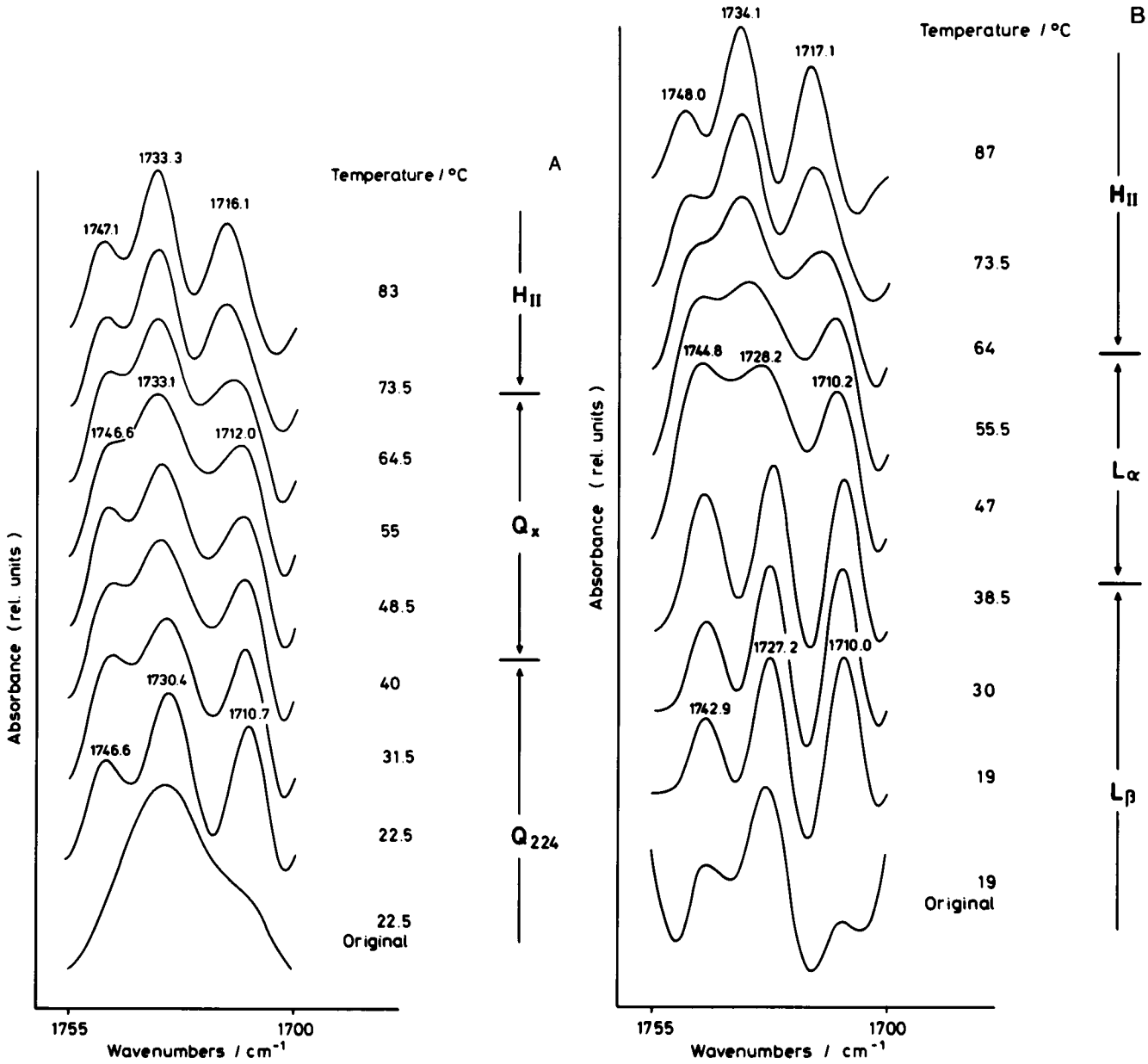

FIGURE 4 Original (*bottom*) and deconvoluted IR spectra in the range of the ester carbonyl stretching vibration $\nu(C{=}O)$ for a LPS R595 preparation at 80% water content at selected temperatures. (*a*) Without Mg^{2+}; (*b*) [LPS]/[Mg^{2+}] = 1:1 M. At the righthand side of the figures, an assignment to the three-dimensional aggregate structures as measured by x-ray diffraction is given for the corresponding temperature ranges (see text). Deconvolution parameters (peakwidth/resolution enhancement factor): 26/1.8.

formation mode (33) of the 3-hydroxy groups within the acyl chains, a phase-specific behavior only of the end-gauche vibration and that due to the formation of kinks is found, i.e., a decrease of the bandwidth at T_c, for example, but no correlation to any structural changes. In contrast, the double-gauche mode, if observed at all, does not exhibit any phase- or structure-specific behavior. Changes in the band position, but not the bandwidth of the 1,324 cm^{-1} vibration, can be correlated with the β- and α-phase states of the acyl chains but not with structural transitions.

Vibrations of the interfacial region

The amide I vibration is superimposed on the strong bending vibration of the aqueous OH groups δ(OH) around 1,645 cm^{-1}. Therefore, measurements also were performed in D_2O (the δ(OD) band lies below the 1,800–1,500-cm^{-1} range). The deconvoluted spectra reveal a splitting into three components (Table 1), which responded only slightly to the acyl chain melting. However, at the $L \leftrightarrow H_{II}$ transition (for the Mg^{2+}-containing sample), the peak position, particularly of the lowest frequency band, was shifted to lower wavenumbers (from

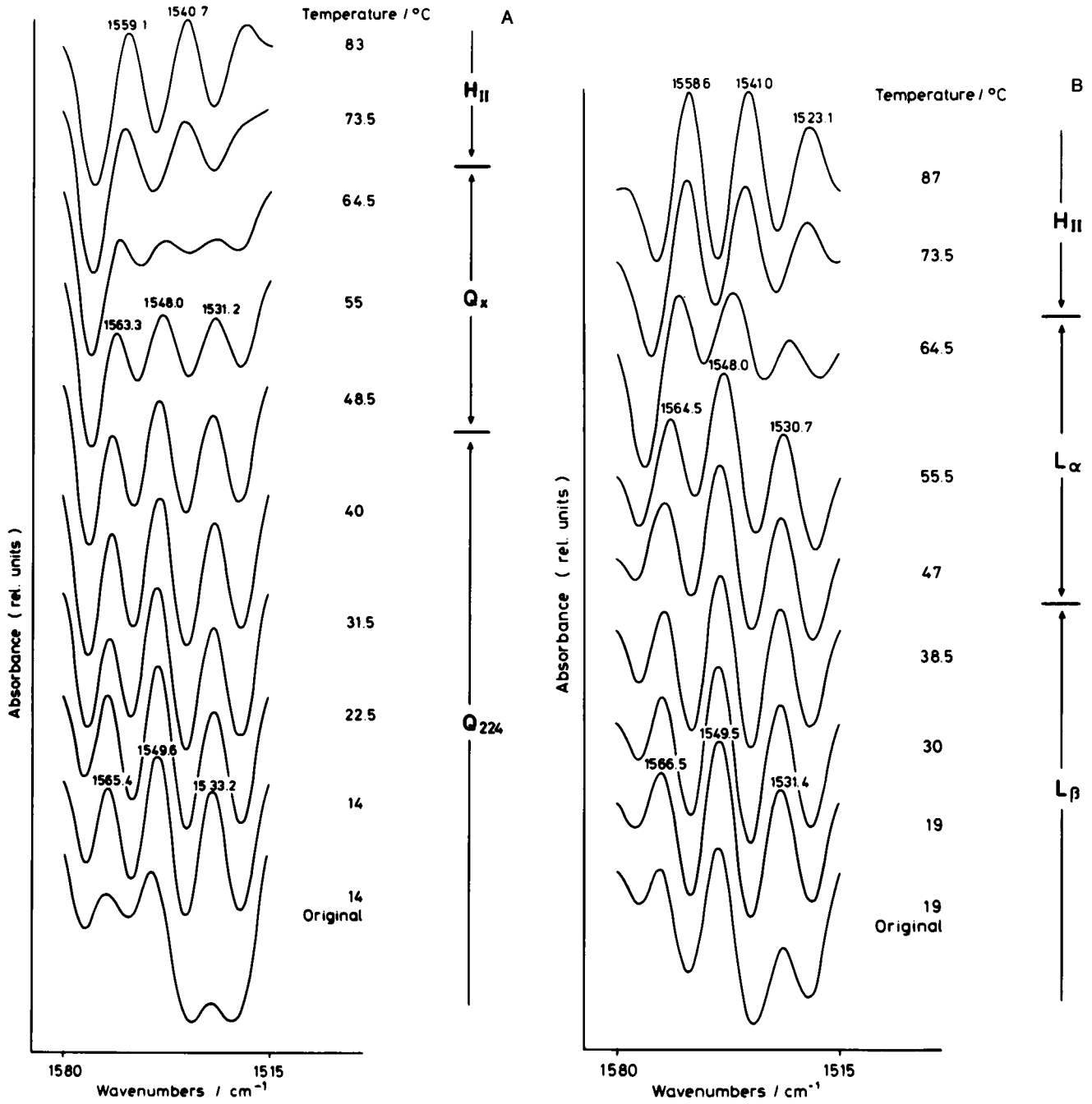

FIGURE 5 Original (*bottom*) and deconvoluted IR spectra in the range of the amide II vibration for a LPS R595 preparation at 80% water content in the temperature range 10–90°C. (*a*) Without Mg^{2+}; (*b*) [LPS]/[Mg^{2+}] = 1:1 M. At the righthand side of the figures, again the assignment to the corresponding three-dimensional aggregate structures is given. Deconvolution parameters: 24/1.65.

1,659 to 1,653 cm^{-1} at T_H), whereas at the cubic to H_{II} transition (for the LPS sample in pure D_2O), practically no changes were registered, i.e., the band position remained at 1,652–1,653 cm^{-1}. It should be noted that all transition temperatures are shifted to higher values (~5°C) due to the exchange of H_2O by D_2O.

A main band at 1,168 cm^{-1} (deconvolution gives a further component at 1,182 cm^{-1}) was formerly attributed to the ester single bond stretching vibration ν(C—O) for phospholipids as well as for LPS (11, 34, 35, 38). Nearly the same bands were found for lipid A (35) and were proposed to consist of a superposition of the ν(C—O) ester band and complex sugar modes. For this band, no characteristic changes of band position, width, and intensity correlating with transitions between phases or structures were observed.

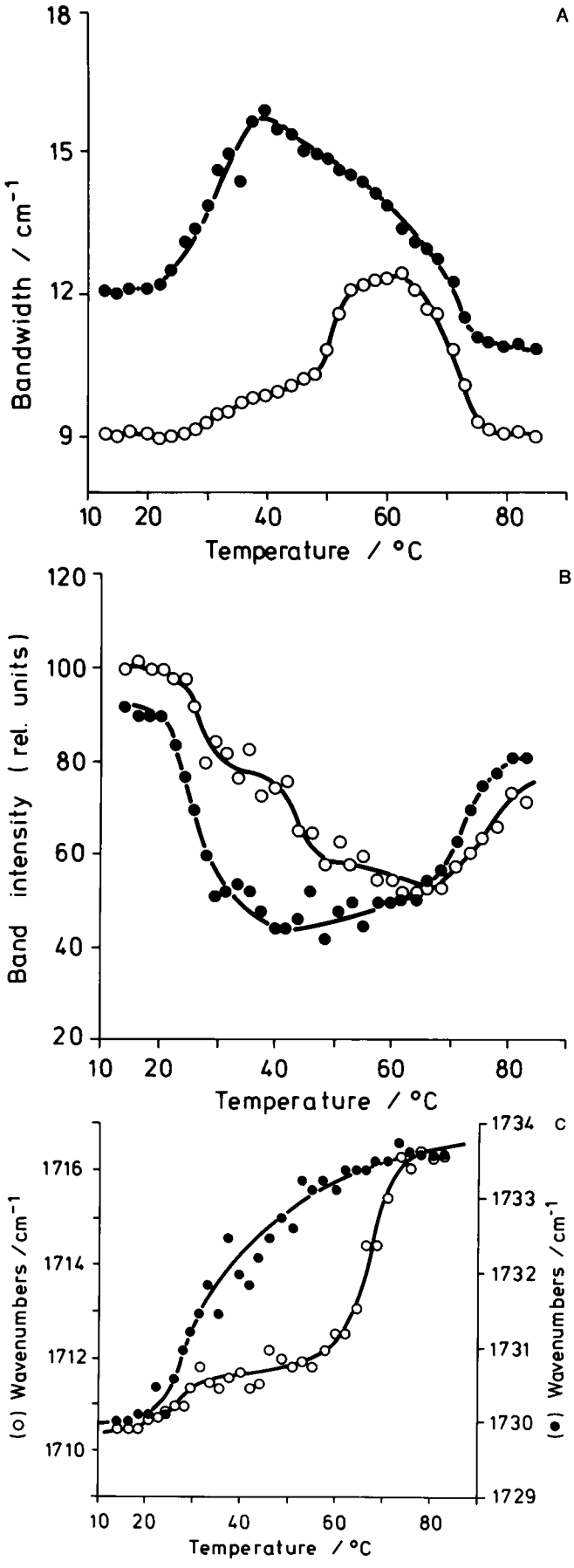

Vibrations from the polar moiety

The antisymmetric stretching vibration of the phosphate $\nu_{as}(PO_2^-)$ at 1,260.0 is shifted to 1,261.3 in the presence of Mg^{2+} and exhibits, similar to the symmetric stretch $\nu_s(PO_2^-)$, only minute changes over the whole temperature range for the band position and width. Only the band intensity shows specific changes at T_c. For the half bandwidth of $\nu_{as}(PO_2^-)$ obtained from the original spectra, absolute values of 22–24 cm^{-1} for the aqueous and 16–19 cm^{-1} for the Mg^{2+}-containing sample were found.

A band at 930 cm^{-1} previously assigned, at least partially, to a vibration connected with the phosphate groups (11) shows considerable fluctuations up to 70°C. The H_{II} structure, however, causes characteristic and reproducible patterns differing for each LPS sample (39).

The deconvoluted spectra in the wavenumber range 1,090–990 cm^{-1} are composed of four to five bands resulting from unspecific vibrations within the sugar moiety and are each characteristic for the Mg^{2+}-free and the Mg^{2+}-containing sample. There is, however, no clear evidence for a correlation with phases or structures.

LPS from *E. coli* F515

The same measurements were performed with a LPS Re sample from *E. coli* strain F515, i.e., again at 80% water content and in the absence and presence of an equimolar content of Mg^{2+}, respectively, and at temperatures between 20 and 80°C. The acyl chain melting behavior is identical to that of LPS R595. The Mg^{2+}-free sample adopts nonlamellar cubic structures, and there seems to be a transition at ~60°C between different cubic phases. The Mg^{2+}-containing sample assumes only lamellar structures. Both preparations exhibit no transition into H_{II} up to a temperature of 80°C. The evaluation of the ester and amide II band contours gave similar characteristics as described above for the acyl chain melting and the transition between different cubic structures. Moreover, parallel to the lack of a transition into H_{II}, absolutely no instances were found for the sharp and characteristic changes at T_H in some of the band parameters presented in Figs. 4–8.

Lipid A from LPS Re of *S. minnesota* and *E. coli*

Further investigations were performed with free lipid A preparations that exhibited a similar structural variability as LPS R595. As an example of this, a lipid A sample

FIGURE 6 Widths (*a*), intensities (*b*), and peak positions (*c*) of the two low frequency ester carbonyl band components versus temperature for a LPS R595 preparation at 80% water content. (●) Band at 1,730 cm^{-1}; (○) band at 1,710 cm^{-1}. The bandwidths in *a* were determined at half height for the 1,730-cm^{-1} band and at 0.75 height for the 1,710-cm^{-1} band, respectively.

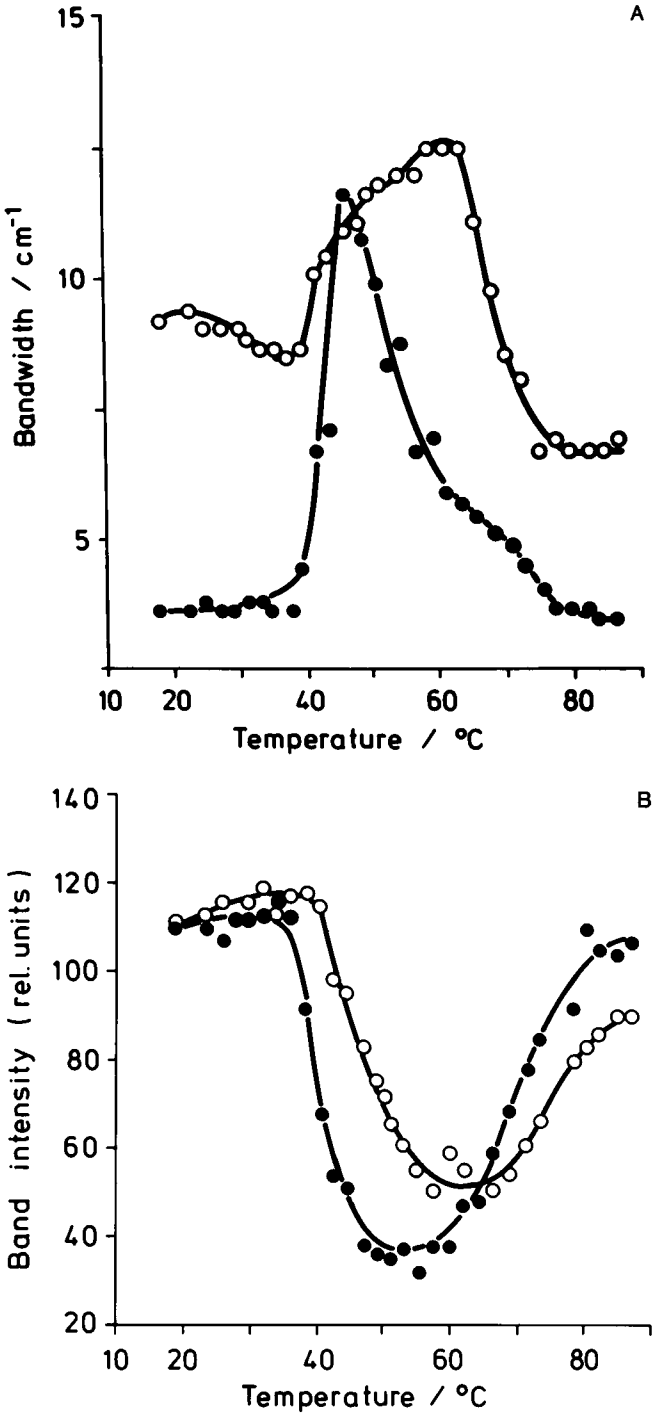

FIGURE 7 Width (*a*) and intensities (*b*) of the two low frequency ester carbonyl band components versus temperature for a LPS R595 preparation at 80% water content and at [LPS]/[Mg^{2+}] = 1:1 M. (●) Band at 1,730 cm^{-1}; (○) band at 1,710 cm^{-1}. The bandwidths in *a* were determined at half height for the 1,710-cm^{-1} band and at 90% height for the 1,730-cm^{-1} band, respectively.

from *E. coli* strain F515 at a water content of 55% in the absence of Mg^{2+} and at a [lipid A]/[Mg^{2+}] molar ratio of 1:2 was analyzed. Again, in a first step the acyl chain melting was determined by monitoring $\nu_s(CH_2)$ as function of temperature. The transition ranges were determined to 37–53°C (T_c = 47°C) and 40–58°C (T_c = 52°C) for the Mg^{2+}-free and Mg^{2+}-containing sample, respectively. The corresponding x-ray spectra are plotted in Fig. 9, *a* and *b* at four selected temperatures. For the lipid A sample in pure water, the analysis shows a coexistence of a lamellar and a cubic structure in the range 20–50°C (e.g., at 40°C, d_l = 4.56 nm; d_Q = 8.63 nm with 3.06 nm = $d_Q/\sqrt{8}$; 2.32 nm = $d_Q/\sqrt{14}$; 1.88 nm = $d_Q/\sqrt{22}$), a pure cubic structure at 60°C (d_Q = 11.1 nm with 7.84 nm = $d_Q/\sqrt{2}$, 4.00 nm = $d_Q/\sqrt{8}$, 2.83 nm = $d_Q/\sqrt{16}$), and a H_{II} structure at 80°C (d_H = 5.68 nm with 3.36 nm = $d_H/\sqrt{3}$, 2.92 nm = $d_H/\sqrt{4}$), whereas the sample with excess Mg^{2+} adopts only lamellar structures but with two periodicities indicating an interdigitated phase (14).

As an example for the temperature dependence of the corresponding IR spectra of the two lipid A preparations, the position and width of the ester band component at 1,710 cm^{-1} are plotted in Fig. 10, *a* and *b*. Again, it seems possible to correlate typical changes of these parameters (also of the band intensity; data not shown), particularly for the LPS sample in pure water to changes in lipid phases and supramolecular structures. Similar to the behavior of the LPS R595 sample (Fig. 6 *c*), the peak position increases only slightly at the $\beta \leftrightarrow \alpha$ but strongly at the cubic to H_{II} transition. In a similar way, analogously to Fig. 6 *a*, the bandwidth increases at the $\beta \leftrightarrow \alpha$ transition and the transition from mixed cubic/lamellar

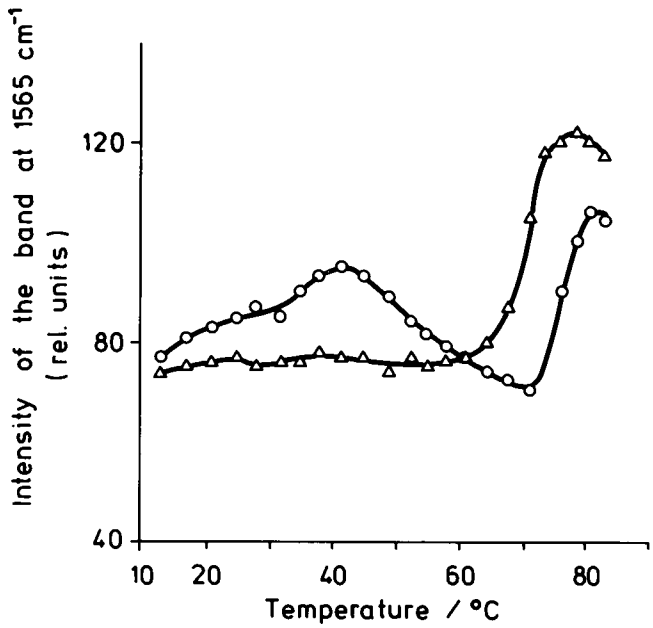

FIGURE 8 Intensities of the amide II band component at 1,565 cm^{-1} versus temperature for a LPS R595 preparation at 80% water content. (○) Without Mg^{2+}; (△) [LPS]/[Mg^{2+}] = 1:1 M.

TABLE 1 **Assignment of different bands found in the IR spectra of LPS Re**

Band numbering*	Tentative assignment of vibration	Approximate peak position after deconvolution
		cm^{-1}
1	Symmetric stretch of methylene groups $\nu_s(CH_2)$	2,850
1	Antisymmetric stretch $\nu_{as}(CH_2)$	2,920
1	Scissoring mode $\delta(CH_2)$	1,467 and 1,485
1	Wagging progression bands $\gamma_w(CH_2)$	1,300–1,180
1	Rocking progression band $\gamma_r(CH_2)$	720
1	Acyl chain conformers double-gauche, end-gauche, and kinks	1,370–1,310
2	Symmetric bending of end methyl $\delta_s(CH_3)$	1,378
2	Antisymmetric stretching $\nu_{as}(CH_3)$	2,955
3	Bending of α-methylene $\delta(\alpha\text{-}CH_2)$	1,415
4	Ester double bond stretch $\nu(C{=}O)$	1,710, 1,730, 1,745
4	Ester single bond stretch $\nu(C{-}O)$‡	1,168 and 1,182
5	Amide I, primarily $\nu(C{=}O)$	1,655, 1,670, 1,685
5	Amide II, primarily $\delta(N{-}H)$	1,530, 1,550, 1,565
6	Antisymmetric stretch of phosphate $\nu_{as}(PO_2^-)$	1,260
6	Symmetric stretch $\nu_s(PO_2^-)$	1,112 and 1,098
6	Unspecific phosphate vibration	930
7	Unspecific sugar vibrations	1,090–990
8	Symmetric carboxylate stretch $\nu_s(COO^-)$	1,412
8	Antisymmetric carboxylate stretch $\nu_{as}(COO^-)$	1,627

The approximations for the peak positions listed in column 3 refer to room temperature and 80% water content (for more detailed information see text).

* See Fig. 1.

‡ Superimposed by an unspecific sugar mode.

to a pure cubic phase and decreases at the cubic to H_{II} transition. In contrast, the position and width of the same band for the sample with excess Mg^{2+} change only slightly over the entire temperature range. For example, a slight decrease of the bandwidth in Fig. 10 *b* seems to indicate the $\beta \leftrightarrow \alpha$ transition. The most important information, however, is the parallelism of invariant lamellar three-dimensional structures (Fig. 9 *b*) with the invariant IR bands (Fig. 10, *a* and *b*), which is not only true for this selected vibration but also for several others particularly resulting from the interface region.

Similar to the situation found for LPS R595, the band contour of the phosphate vibrations, particularly of $\nu_{as}(PO_2^-)$, is temperature invariant for both preparations (data not shown). However, the half bandwidths differ, giving values of 17–18 cm^{-1} for the Mg^{2+}-free sample and 15–16 cm^{-1} for the Mg^{2+}-containing sample, which, thus, are significantly lower and lie closer together as compared with LPS R595.

The analysis was completed by measurements at extremely high water content (under near physiological conditions), i.e., at 99.5% D_2O content, which is far beyond the measurability by x-ray small-angle diffraction. Lipid A from *S. minnesota* strain R595 was chosen for which a complete phase diagram was established recently (14). For this compound, at low and medium water concentrations the $\beta \leftrightarrow \alpha$ acyl chain melting is coupled with a transition into H_{II}, i.e., these two processes proceed simultaneously (between 48 and 63°C). At the highest water concentrations (>80%), however, the beginning of the transition into H_{II} starts at ~65°C after completion of the $\beta \leftrightarrow \alpha$ chain melting (40–55°C), i.e., these two processes are decoupled. In control experiments at a water content of 80%, it turned out that the results of the IR measurements have similar characteristics as those described above for LPS R595 and for lipid A from *E. coli* (except that the transitions are shifted 5°C higher because of the exchange of H_2O by D_2O). A detailed evaluation of the low frequency component of the ester carbonyl stretching bands shows that at these extremely high water concentrations the band positions change dramatically compared with lower water contents, i.e., are shifted from 1,710 to 1,714 to 1,716 cm^{-1} in the gel state of the hydrocarbon chains. Moreover, in the presence of Mg^{2+}, the main component of the ester vibration usually lying at ~1,730 cm^{-1} split into two components at 1,724 and 1,735 cm^{-1}, respectively. From the evaluation of the band intensity and width, however, again correlations to structural changes seem to be possible. For example, the intensity of the lowest frequency ester band is plotted versus temperature (Fig. 11). It exhibits a strong decrease at 45–58°C that might be connected with an acyl chain melting and/or a transition between different cubic structures and an increase at 65–75°C, probably due to the transition into H_{II}. The amide vibrations behave similarly, e.g., the band components lying at 1,572, 1,542 and at 1,683 cm^{-1} (data not shown).

Specific vibrations of LPS Re

A careful comparison of the IR spectra of dehydrated free lipid A and LPS Re shows significant higher absorbance in the wavenumber range 1,100–1,000 cm^{-1} for LPS Re that should be due to unspecific vibrations within the 2-keto-3-deoxyoctonate sugar moiety. Absorption bands at ~1,412 and 1,627 cm^{-1} that are existent to a significant degree only for LPS Re allow an assignment to the symmetric and antisymmetric stretching mode of the COO^- (carboxylate) groups, respectively, within the 2-keto-3-deoxyoctonate moiety of

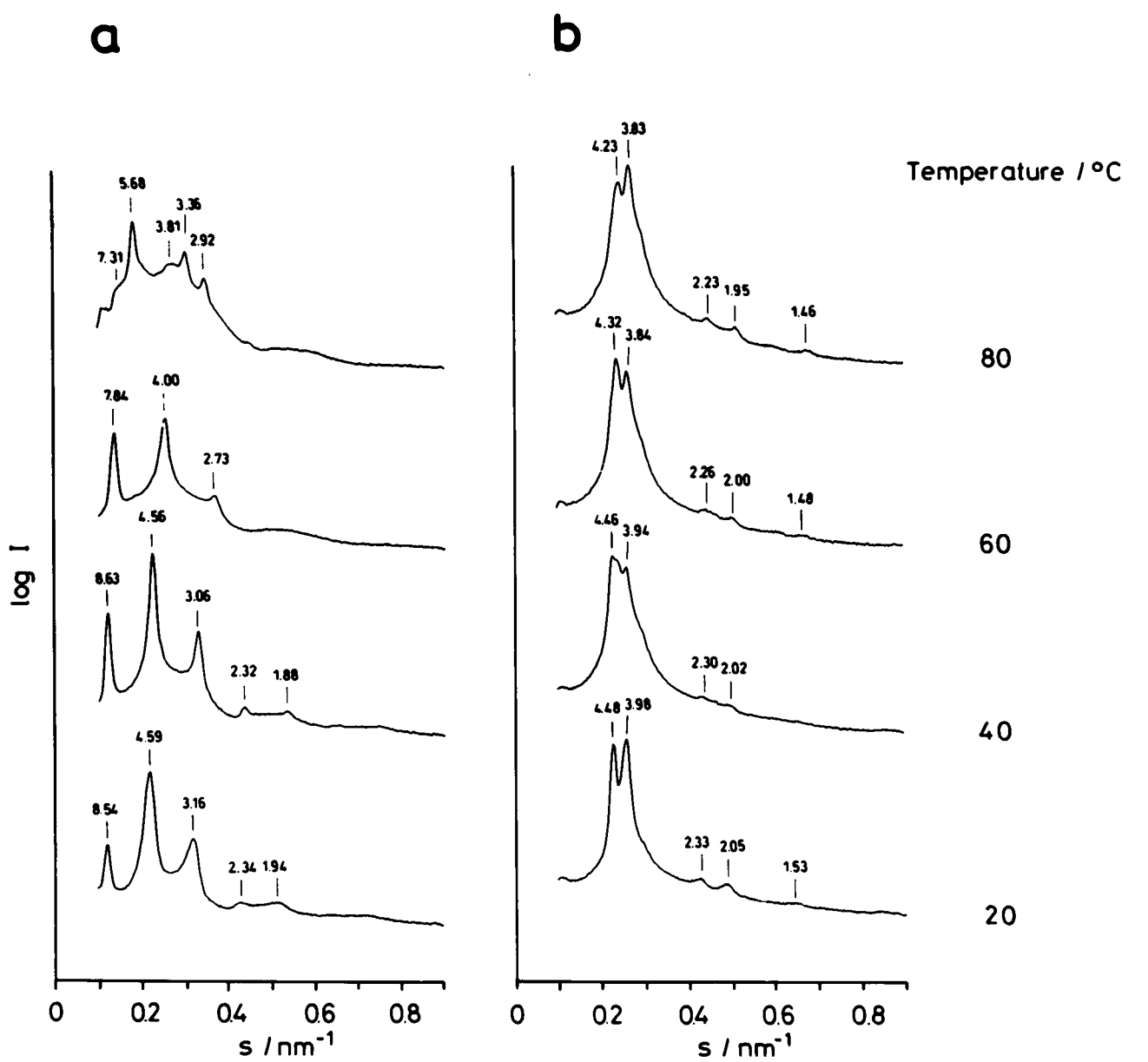

FIGURE 9 Small-angle X-ray diffraction patterns for free lipid A from *E. coli* F515 at four selected temperatures and at 55% water content. (*a*) Without Mg^{2+}; (*b*) [lipid A]/[Mg^{2+}] = 1:2 M. The listed spacings are in nm.

LPS. The band contour of $\nu_{as}(COO^-)$ reacts only slightly at the Q ↔ H_{II} transition by changes particularly in peak position but strongly at the L ↔ H_{II} transition, where a splitting occurs into two band components around 1,633 and 1,619 cm^{-1}, respectively (data not shown). To test a possible protonation of the carboxylate groups around neutral pH, the acyl chain melting behavior was checked similar to that reported in Brandenburg and Seydel (6), allowing to establish the positions of pK_a's. At pH 5–9, only slight variations of T_c were found; however, at pH 2–4 a significant increase and at pH 9–10 a decrease of T_c were observed. From these results, it may be deduced that pK_a's should lie between 4–5 and 9–10, respectively. A more detailed analysis of the pH dependence of this spectral range yields a vanishing of the 1,627 cm^{-1}-band at pH 3, i.e., both carboxylate groups are protonated, whereas at pH 4–11 no change of this band can be noticed. In the basic pH range (at ~pH 9.5), a change of the band contour of $\nu_{as}(PO_2^-)$ indicates a change in the protonation of the phosphate group. Therefore, in the neutral pH range both carboxylate groups seem to be deprotonated.

A band component between 1,420 and 1,400 cm^{-1} results from the bending vibration of the α-methylene groups $\delta(\alpha\text{-}CH_2)$ and is superimposed on $\nu_s(COO^-)$. For LPS Re the change of the band contours in the wave-

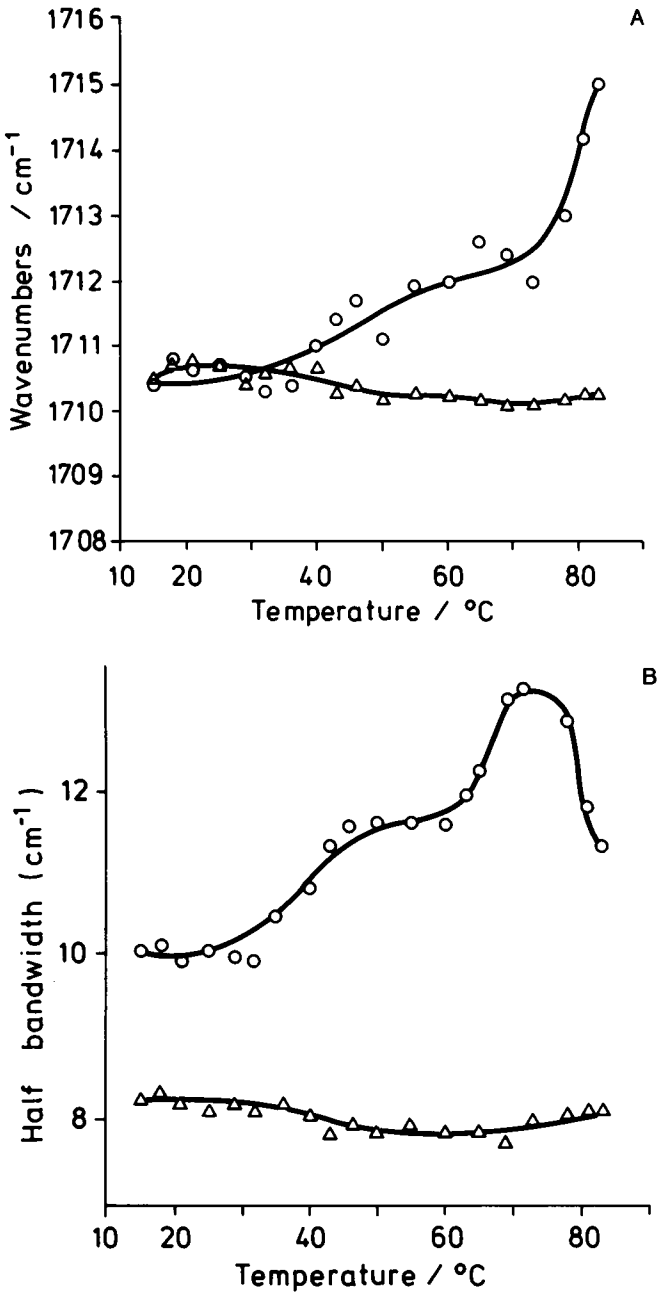

FIGURE 10 Peak position (*a*) and half bandwidth (*b*) of the lowest frequency ester carbonyl band component for free lipid A from *E. coli* F515 at 55% water content. (○) Without Mg^{2+}; (△) [lipid A]/[Mg^{2+}] = 1:2 M.

number range 1,450–1,390 cm^{-1} as function of temperature clearly indicates the transition into H_{II} in that the single components around 1,405–1,401 and 1,415–1,410 cm^{-1} shift drastically to higher values at T_H. Furthermore, similar to other vibrational bands presented above, the half width of the latter band component changes significantly for the Q to H_{II} and much stronger for the L to H_{II} transitions (in both cases a band broadening takes place). In contrast, the bands at 1,400 and 1,418 cm^{-1} found for lipid A do not show any significant changes between 20 and 80°C. Therefore, the shifts of the peak positions and the half bandwidths are due to changes within the carboxylate group, whereas the band contour of the bending vibration $\delta(\alpha\text{-}CH_2)$, although located in the interface region, is not influenced by structural transitions.

DISCUSSION

Enterobacterial bisphosphoryl lipid A and deep rough mutant LPS exhibit an extremely complex structural polymorphism, i.e., the state of order of the acyl chains and the three-dimensional structures adopted in an aqueous environment strongly depend on water content, Mg^{2+} concentration, and temperature (4). At low water concentrations (<50%) and, independently of water content, at a lipid/Mg^{2+} ratio of 1 or lower, only lamellar structures were found (7, 10, 13–15). Above 50% water concentration, preferentially nonlamellar or mixed lamellar/nonlamellar structures can be observed at Mg^{2+} concentrations below equimolarity (see Figs. 3 *a* and 9 *a*; [4, 8, 13–15]). Free lipid A and deep rough mutant LPS Re from *S. minnesota* R595, moreover, adopt at higher temperatures, starting between 55 and 70°C, hexagonal II structures (Figs. 3 and 9 *a*), whereas for LPS Re from *E. coli* F515 and for other rough mutant LPS Rd to Ra from *S. minnesota,* this transition is not observed (15, Seydel, U., M. H. J. Koch, and K. Brandenburg, unpublished results). Most importantly, under near physiological conditions (high water contents and at 37°C), free

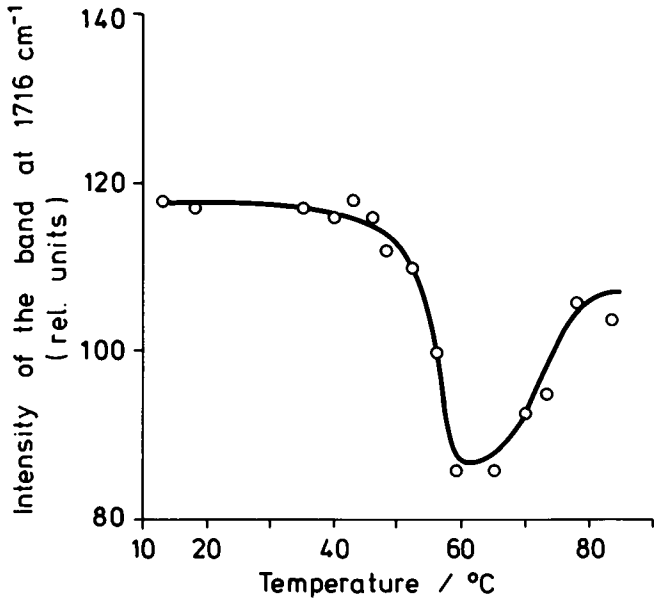

FIGURE 11 Intensity of the lowest frequency ester carbonyl band component versus temperature for free lipid A from *S. minnesota* R 595 at 99.5% D_2O content.

lipid A and LPS Re tend to form three-dimensional structures with cubic symmetry. This was extensively discussed previously and could be correlated with the potency of these molecules to induce a variety of biological effects in mammals (4, 8, 14), supporting the view of Luzzati et al. (27, 28) and others (40–43) of the general biological importance of cubic structures in amphiphile/water systems. The fact that for the Mg^{2+}-free samples, cubic structures are found above as well as below T_c, i.e., also in the ordered (β) phase (Figs. 3 *a* and 9 *a*), is a very new finding and was discussed recently (14, 15). As an explanation the partial "fluidization" of the acyl chains measured by IR and differential scanning calorimetry was proposed, allowing the chain segments particularly near the end methyl groups to be much more flexible than those of comparable phospholipids in the same phase state. In this way, more complex than pure lamellar structures may be adopted. Interestingly, some preliminary x-ray measurements at temperatures < 0°C show that LPS Rs and free lipid A now adopt a multibilayered organization (Seydel, U., and K. Brandenburg, unpublished data).

Because of this high structural variability of free lipid A and LPS R595, proven with small-angle x-ray diffraction, they seemed to be particularly suitable for a comparative analysis applying x-ray and IR spectroscopy. The results clearly demonstrate the ability of the IR technique to detect changes of the supramolecular arrangements via monitoring certain vibrational bands. Generally, it can be stated that the single-band components respond differently to structural reorientations and are influenced, also independently of the particular supramolecular structure adopted, by variations of water content, Mg^{2+}, and by the chemical structure. This holds true especially for the band positions, i.e., from the absolute values of the ester bands, for example, a differentiation between the influences of water, Mg^{2+}, and/or the supramolecular structure is not possible. The band intensities and widths, however, allow a more straightforward differentiation between structural influences and those of ambient parameters.

Bands from the interfacial region

The vibrational bands resulting from the hydrophilic/hydrophobic interface region are excellently suitable to demonstrate the correlation of x-ray diffraction and deconvoluted FT-IR data, with respect to a characterization of the phase states and the different lamellar and nonlamellar structures. This is exemplarily shown in Figs. 3–5 for the LPS/water and LPS/water/Mg^{2+} samples, respectively. The extent of the supramolecular reorientations has a direct impact on the IR band parameters, i.e., changes of the band parameters are much more strongly expressed for the $L \leftrightarrow H_{II}$ than for the $Q \leftrightarrow H_{II}$ transition and lowest for the cubic $\leftrightarrow$ cubic transitions. This becomes evident when comparing the changes in band intensity for the ester bands ($Q \leftrightarrow H_{II}$, Fig. 6 *b*, and $L \leftrightarrow H_{II}$, Fig. 7 *b*), the amide II bands (Fig. 8) and the carboxylate bands at 1,410 and 1,627 cm^{-1} (Q to H_{II} and L to H_{II}, respectively), and for the 1,710-cm^{-1} ester band and the amide II band (both cubic $\leftrightarrow$ cubic transitions; Figs. 6 *a* and 8).

For a better understanding of the mechanisms accompanying the structural transitions, the characterization of the structure-sensitive vibrations on a molecular level should provide a deeper insight. For this, literature data for phospholipids might be useful, especially in the range of the ester carbonyl stretching vibration. However, the single components of the C=O ester band contour result from complex superposition of hydration effects, contributions of the single acyl chain conformations, and from the whole bilayer (44). For diacyl phospholipids, two band components were assigned to the *sn*-1 and *sn*-2 acyl chains, respectively, having different conformations (45–47), and a third band component was attributed to an overlapping of C=O vibrational bands of neighboring molecules (48). A splitting of the ester ν(C=O) band contour due to different hydrogen binding of the two C=O groups was first proposed by Fringeli (38) in his pioneering work on IR dichroic measurements of various phospholipids. A similar assignment to strong and weak hydrogen binding was performed also for dimyristoyl phosphatidylserine (49). This was confirmed by Blume et al. (32) for the negatively charged dimyristoyl phosphatidic acid: splitting of the carbonyl bands occurs only when hydrogen bonding is possible between the ester groups and the solvent, leading to a low frequency due to hydrogen bonding and a high frequency contribution due to the free carbonyls but independently of the chain bearing the C=O group.

A splitting into three band components was found, especially for negatively charged phospholipids (49, 50). For enterobacterial endotoxins, a similar splitting of the bands into three components is observed, although the molecular architecture of these molecules is quite different from that of diacyl phospholipids. The former carry in general one double and three single esters, i.e., five carbonyl C=O bonds. The splitting occurs even in "dehydrated" LPS samples prepared from an organic solvent; however, in these preparations there is still a remainder of 5–10% water content. The degree of splitting of the ester carbonyl bands is nearly unaffected by addition of Mg^{2+} (Fig. 4). Comparison of the peak positions of the Mg^{2+}-free and Mg^{2+}-containing sample shows, however, that the two higher frequency components are most affected by addition of Mg^{2+}, resulting in a reduction from 1,746.5 to 1,742.9 cm^{-1} and from 1,729.9 to 1,727.2 cm^{-1} at the lowest temperature. For an interpretation of this effect, it should be noted that for LPS R595 recently, stronger binding of water in the presence of Mg^{2+} was found, which was proven by differential scanning calorimetry of free and bound water (15). More-

over, for hydrated LPS samples in saturated water vapor, two sharp IR bands centered at 3,320 and 3,350 cm^{-1}, which can be attributed to intermolecular bound water, were observed only in the presence of Mg^{2+} (Brandenburg, K., unpublished results). From these data it can be concluded that (*a*) the structural rearrangement from cubic to lamellar is accompanied by an increasing bonding and alignment of water molecules, in agreement with the higher overall order of the lamellar structures, and (*b*) the kind and degree of splitting of the ester C=O band contour essentially depends on the magnitude of hydrogen bonding in the interface region but not at all on the number of single C=O groups.

Increased hydrogen bonding in the presence of cations like Ca^{2+} and Mg^{2+} was also found for negatively charged phospholipids (49–51). However, whether the addition of divalent cations was accompanied by structural transitions as observed here for endotoxins was not investigated in these reports except by Laroche et al. (50), who did not find changes of the lamellar structure for dimyristoyl phosphatidic acid upon addition of Ca^{2+}.

Interestingly, for both LPS samples in the H_{II} structure, the band positions and shapes of the three components are quite similar. This, again, indicates an interrelationship between hydration of the ester groups and the supramolecular structures of the LPS assemblies.

Mantsch et al. (20, 21) investigated the temperature-governed structural sequence $L_\beta \leftrightarrow L_\alpha \leftrightarrow H_{II}$ of PE from natural sources. As may be expected from the foregoing discussion, the absolute values and the temperature dependence of the peak positions are different from the results for endotoxins. However, an excellent accordance with the $L_\beta \leftrightarrow L_\alpha \leftrightarrow H_{II}$ transition of LPS Re (Fig. 3 *b*) is found for the changes in width of the ester carbonyl bands: an increase at the lamellar $\beta \leftrightarrow \alpha$ and a decrease at the transition into H_{II} with values for the half bandwidths being very similar below T_c and above T_H (Fig. 7 *a*).

Bands from the hydrophobic and hydrophilic moiety

Most of the band contours of IR vibrations resulting from the pure polar and apolar moieties, respectively, do not display a noticable dependence on the three-dimensional structures. However, as shown previously in comprehensive analyses of phospholipids (18, 19, 52), some bands from the hydrophobic moiety are excellent indicators of the state of order of the hydrocarbon chains, particularly $\nu_s(CH_2)$ and $\nu_{as}(CH_2)$. The small changes observed here for the $\nu_s(CH_2)$ vibration (Fig. 2) at 65–75°C, i.e., around T_H, do not indicate the transition to H_{II} reliably, because similar changes in the peak position of $\nu_s(CH_2)$ were also observed for other rough mutant LPS undergoing no transition into H_{II}. The only exception with respect to structural sensitivity is the scissoring band $\delta(CH_2)$ that indicates, besides the transition between the β and α state, also that to the H_{II} structure. The band contours of all other acyl chain modes—like the conformers double-gauche, end-gauche, and kink sequences—the rocking modes $\gamma_r(CH_2)$, the bending δ_s, and stretching vibration ν_{as} of CH_3 do not detect structural rearrangements; even the acyl chain melting is not or only poorly expressed. The invariance of the latter vibrations was also observed for phospholipids (e.g., by Mendelsohn et al. (53) and Casal and McElhaney (37), who used the invariance of a particular rocking mode in deuterated samples and of $\delta_s(CH_3)$, respectively) in dipalmitoyl phosphatidylcholine preparations for an absolute determination of the conformational disorder within the acyl chains.

The phosphate vibrational bands ν_s and $\nu_{as}(PO_2^-)$ are nearly invariant for the different samples and structures. This is surprising since it is assumed that divalent cations bridge adjacent LPS molecules via binding to these groups (54). However, the available data on phospholipids are in full accordance with our observations, e.g., no influence of the peak positions of ν_s and $\nu_{as}(PO_2^-)$ on the L_β, L_α, and H_{II} structures of natural PE was found (55, 56). These findings were confirmed in a recent report (57) for the $L_\alpha \leftrightarrow H_{II}$ transition of dioleoyl phosphatidylethanolamine. From observations like these, Casal and Mantsch (18) concluded that the headgroups are nearly unaffected by the transition from the lamellar to the nonbilayer H_{II} phase and that the general conformation and the degree of hydration in the phases are quite similar.

The absolute values 1,260 cm^{-1} for $\nu_{as}(PO_2^-)$ are drastically higher than for phospholipids, for which they are found at 1,220 in hydrated (phosphatidylcholine) and 1,240 cm^{-1} for weakly hydrated (PE) systems (34, 52). This suggests that the phosphate groups of lipid A and LPS are extremely dehydrated in contrast to other bands of the polar or interface region and in agreement with the observation that Mg^{2+} has only a slight influence on the bandwidth of $\nu_{as}(PO_2^-)$ but not on the peak position. However, the chemical environment of the phosphate groups in LPS/lipid A is different from that in PE or phospatidylcholine. The negatively charged compound phosphatidic acid, bearing the phosphate group in the terminal position, should be more suitable for a comparison. For hydrated dimyristoyl and dioleoyl phosphatidic acid, we found the peak position of $\nu_{as}(PO_2^-)$ around 1,252 cm^{-1} (K. Brandenburg, unpublished data). This indicates that the absolute values for the peak position of $\nu_{as}(PO_2^-)$ are, already in phospholipids, dependent on the chemical composition.

The absolute values of the bandwidths are, however, very different for lipid A and LPS Re, the former having significantly lower values. As the bandwidth monitors the freedom of motion of the absorbing groups and with that the amplitudes and rates of motion within its immediate environment, the phosphate groups of free lipid A

seem to be motionally significantly more restricted than those of LPS Re despite the basically identical supramolecular structure. The lower mobility of the phosphate groups within the free lipid A molecules might be the reason for the recent finding that anti-lipid A antibodies reacted much more strongly with lipid A incorporated in phospholipid liposomes than with it in free form, whereas the corresponding data for LPS R595 gave no difference between the endotoxin incorporated in liposomes and in free form (58). However, this interpretation should not be overemphasized because different substitution of the two endotoxins with arabinose, for example, (see Fig. 1) in nonstochoimetric amounts might lead to different chemical environments of the respective phosphate groups resulting in undefinite changes of the bandwidth.

Only limited data are available for a comparison of the results on endotoxins, i.e., those of Naumann et al. (7, 35) for the lipid A/water and LPS Re/water systems. In contrast to the corresponding data shown here, these authors found only lamellar structures in the temperature range 10–60°C. This disagreement might possibly be due to the distinct lyotropic behavior of endotoxins, i.e., the water content of the samples investigated by Naumann et al. were "fully hydrated" (a definite lipid/water ratio was not given) and might therefore not exceed a value of 50% water content, which was found to be the lower limit for the occurrence of nonlamellar structures (14, 15). Considering the IR spectroscopic measurements, the results from the evaluation of some vibrations from the hydrophobic moiety, particularly $\nu_s(CH_2)$, are in full accordance with the present investigation. A direct comparison to the behavior of vibrations from the interface region, i.e., the ester carbonyl stretching bands is not possible in a straightforward way due to the lack of knowledge of the precise water content. However, the behavior of the peak position of the lowest frequency ester band for aqueous lipid A was reported to be at least qualitatively similar to our observations (Fig. 10 *a*), i.e., in Naumann et al. (35), above T_c a jump in the peak position from 1,712.0 to 1,717.0 cm^{-1} was found.

CONCLUSIONS

The approach of this article was to correlate x-ray spectroscopically determined supramolecular structures of endotoxins with characteristics of various IR bands originating from different regions of the molecules. It could be shown that supramolecular reorientations lead to changes, particularly in the band position of vibrations from the interfacial region, but that changes in ambient parameters might cause the same effect. However, the behavior of band intensities and widths allow a clearer differentiation between the influence of a pure change of ambient parameters and a concomitant change in the physical three-dimensional structure.

The relative invariance of the phosphate vibrations is of special interest. It is known that the phosphate groups are essential for the biological activity of endotoxins (2) and that they display, furthermore, characteristic antibody specificities (58). Therefore, a more detailed study of the interrelationship between the biological reactivity, the supramolecular conformations, and the mobility of the phosphate groups of endotoxins might provide further insight in the interaction mechanisms.

Furthermore, the determination of absolute band parameters, particularly of vibrations from the interface region for different endotoxin preparations that also includes those with a more complete core oligosaccharide (LPS from Rd to Ra mutants), should be subject to further studies applying curve-fitting procedures of the original spectra after deconvolution (32), thus allowing the precise reconstitution of the original spectra.

The results of this study should be confirmed in further investigations also on phospholipids allowing a direct structural determination without the need of x-ray diffraction measurements. This would be highly advantageous because IR measurements can be performed quickly, are applicable over a wide range of water content, and, most importantly, require only small sample amounts.

I am indebted to Drs. M. H. J. Koch, U. P. Fringeli, and, particularly, U. Seydel for critically reading the manuscript and many helpful discussions. I also thank Ms. H. Lüthje for the extraction of LPS and isolation of lipid A preparations, Ms. M. Lohs for preparing the drawings, and Ms. G. Stegelmann for the photographs.

Received for publication 5 October 1992 and in final form 2 December 1992.

REFERENCES

1. Lüderitz, O., M. A. Freudenberg, C. Galanos, V. Lehmann, E. Th. Rietschel, and D. H. Shaw. 1982. Lipopolysaccharides of Gram-negative bacteria. *Curr. Top. Membr. Transp.* 17:79–151.
2. Rietschel, E. Th., L. Brade, U. Schade, U. Seydel, U. Zähringer, S. Kusumoto, and H. Brade. 1988. Bacterial endotoxins: properties and structure of biologically active domains. *In* Surface Structures of Microorganisms and Their Interaction with the Mammalian Host. E. Schrinner, M. H. Richmond, G. Seibert, and U. Schwarz, editors. Verlag Chemie, Weinheim, Germany. 1–41.
3. Rietschel, E. Th., T. Kirikae, H. Loppnow, P. Zabel, A. J. Ulmer, H. Brade, U. Seydel, U. Zähringer, M. Schlaak, H.-D. Flad, and U. Schade. 1991. Molecular aspects of the chemistry and biology of endotoxin. *In* Molecular Aspects of Inflammation. H. Sief, L. Floh'e, and G. Zimmer, editors. Springer-Verlag, Berlin/Heidelberg/New York/Tokyo. 207–231.
4. Seydel, U., and K. Brandenburg. 1992. Supramolecular structure of lipopolysaccharides and lipid A. *In* Bacterial Endotoxic Lipopolysaccharides. Vol. I. *Molecular Biochemistry and Cellular Biology.* D. C. Morrison and J. Ryan, editors. CRC Press, Bota Raton, FL. 225–250.
5. Brandenburg, K., and U. Seydel. 1984. Physical aspects of struc-

ture and function of membranes made from lipopolysaccharides and free lipid A. *Biochim. Biophys. Acta.* 775:225–238.

6. Brandenburg, K., and U. Seydel. 1990. Investigation into the fluidity of lipopolysaccharide and free lipid A membrane systems by Fourier-transform infrared spectroscopy and differential scanning calorimetry. *Eur. J. Biochem.* 191:229–236.
7. Naumann, D., C. Schultz, A. Sabisch, M. Kastowsky, and H. Labischinski. 1989. New insights into the phase behaviour of a complex anionic amphiphile: architecture and dynamics of bacterial deep rough lipopolysaccharide membranes as seen by FTIR, X-ray, and molecular modelling techniques. *J. Mol. Struct.* 214:213–246.
8. Seydel, U., K. Brandenburg, M. H. J. Koch, and E. Th. Rietschel. 1989. Supramolecular structure of lipopolysaccharide and free lipid A under physiological conditions as determined by synchrotron small-angle X-ray diffraction. *Eur. J. Biochem.* 186:325–332.
9. Coughlin, R. T., A. A. Peterson, A. Haug, H. J. Pownall, and E. J. McGroarty. 1985. A pH titration study on the ion binding within lipopolysaccharide aggregates. *Biochim. Biophys. Acta.* 821:404–412.
10. Labischinski, H., G. Barnickel, H. Bradaczek, D. Naumann, E. Th. Rietschel, and P. Giesbrecht. 1985. High state of order of isolated bacterial lipopolysaccharide and its possible contribution to the permeation barrier property of the outer membrane. *J. Bacteriol.* 162:9–20.
11. Brandenburg, K., and U. Seydel. 1988. Orientation measurements on membrane systems made from lipopolysaccharides and free lipid A by FT-IR spectroscopy. *Eur. Biophys. J.* 16:83–94.
12. Labischinski, H., E. Vorgel, W. Uebach, R. P. May, and H. Bradaczek. 1990. Architecture of bacterial lipid A in solution. A neutron scattering small-angle scattering study. *Eur. J. Biochem.* 190:359–363.
13. Seydel, U., and K. Brandenburg. 1990. Conformations of endotoxin and their relationship to biological activity. *In* Cellular and Molecular Aspects of Endotoxin Reactions. A. Nowotny, J. J., Spitzer, and E. J. Ziegler, editors. Elsevier, Amsterdam. 61–71.
14. Brandenburg, K., M. H. J. Koch, and U. Seydel. 1990. Phase diagram of lipid A from *Salmonella minnesota* and *Escherichia coli. J. Struct. Biol.* 105:11–21.
15. Brandenburg, K., M. H. J. Koch, and U. Seydel. 1992. Phase diagram of deep rough mutant lipopolysaccharide from *Salmonella minnesota* R595. *J. Struct. Biol.* 108:93–106.
16. Cullis, P. R., B. de Kruijff, M. J. Hope, A. J. Verkleij, R. Nayar, S. W. B. Farren, C. Tilcock, T. D. Madden, and M. B. Bally. 1983. Structural properties of lipids and their functional roles in biological membranes. *In* Membrane Fluidity in Biology. Vol. 1. Concepts of Membrane Structure. R. C. Aloia, editor. Academic Press, New York. 39–81.
17. Tilcock, C. P. S., P. R. Cullis, and S. M. Gruner. 1986. On the validity of ^{31}P-NMR determination of phospholipid polymorphic phase behaviour. *Chem. Phys. Lipids.* 40:47–56.
18. Casal, H. L., and H. H. Mantsch. 1984. Polymorphic phase behaviour of phospholipid membranes studied by infrared spectroscopy. *Biochim. Biophys. Acta.* 779:381–401.
19. Mantsch, H. H., and R. N. McElhaney. 1991. Phospholipid phase transitions in model and biological membranes as studied by infrared spectroscopy. *Chem. Phys. Lipids.* 57:213–226.
20. Mantsch, H. H., A. Martin, and D. G. Cameron. 1981. Characterization by infrared spectroscopy of the bilayer to nonbilayer phase transition of phosphatidylethanolamines. *Biochemistry.* 20:3138–3145.
21. Mantsch, H. H., A. Martin, and D. G. Cameron. 1981. An infrared spectroscopic characterization of the polymorphic phase behaviour of human erythrocyte phosphatidylethanolamine. *Can. J. Spectrosc.* 26:79–84.
22. Galanos, C., O. Lüderitz, and O. Westphal. 1969. A new method for the extraction of R lipopolysaccharides. *Eur. J. Biochem.* 9:245–249.
23. Brade, H., C. Galanos, and O. Lüderitz. 1983. Differential determination of the 3-deoxy-D-mannooctulosonic acid residues in lipopolysaccharides of *Salmonella minnesota* rough mutants. *Eur. J. Biochem.* 131:195–200.
24. Koch, M. H. J., and J. Bordas. 1983. X-ray diffraction and scattering on disordered systems using synchrotron radiation. *Nucl. Instrum. Methods.* 208:461–469.
25. Gabriel, A. 1977. Position-sensitive X-ray detector. *Rev. Sci. Instrum.* 48:1303–1305.
26. Boulin, C., R. Kempf, M. H. J. Koch, and S. M. Laughlin. 1986. Data appraisal evaluation and display for synchrotron radiation experiments: hardware and software. *Nucl. Instrum. Methods.* A249:399–407.
27. Luzzati, V., A. Gulik, T. Gulik-Krzywicki, and A. Tardieu. 1986. Lipid polymorphism revisited: structural aspects and biological implications. *In* Lipids and Membranes: Past, Present, and Future. J. A. F. Op den Kamp, B. Roelofson, and K. W. A. Wirtz, editors. Elsevier, Amsterdam. 137–151.
28. Luzzati, V., P. Mariani, and T. Gulik-Krzywicki. 1987. The cubic phases of liquid-containing systems: physical structure and biological implications. Physics of amphiphilic layers. *Springer Proc. Phys.* 21:131–137.
29. Kauppinen, J. K., D. J. Moffat, H. H. Mantsch, and D. G. Cameron. 1981. Fourier self-deconvolution: a method for resolving intrinsically overlapped bands. *Appl. Spectrosc.* 35:271–276.
30. Cameron, D. G., and D. J. Moffat. 1984. Deconvolution, derivation, and smoothing of spectra using Fourier transforms. *J. Testing Evaluation.* 12:78–85.
31. Mantsch, H. H., H. L. Casal, and R. N. Jones. 1986. Resolution enhancement of infrared spectra of biological systems. *In* Spectroscopy of Biological Systems. J. H. Clark and R. E. Hester, editors. John Wiley and Sons, New York. 1–46.
32. Blume, A., W. Hübner, and G. Messner. 1988. Fourier transform infrared spectroscopy of $^{13}C{=}O$ labeled phospholipids hydrogen bonding to carbonyl groups. *Biochemistry.* 27:8239–8249.
33. Bellamy, L. J. 1975. The Infrared Spectra of Complex Molecules. Chapman and Hall, London. 433 pp.
34. Fringeli, U. P., and Hs. H. Günthard. 1981. Infrared membrane spectroscopy. Membrane spectroscopy. *Mol. Biol. Biochem. Biophys.* 31:270–332.
35. Naumann, D., C. Schultz, J. Born, H. Labischinski, K. Brandenburg, G. von Busse, H. Brade, and U. Seydel. 1987. Investigations into the polymorphism of lipid A from lipopolysaccharides of *Escherichia coli* and *Salmonella minnesota* by Fourier-transform infrared spectroscopy. *Eur. J. Biochem.* 164:159–169.
36. Maroncelli, M., S. P. Qi, H. L. Strauss, and R. G. Snyder. 1982. Nonplanar conformers and the phase behaviour of solid *n*-alkanes. *J. Am. Chem. Soc.* 104:6237–6247.
37. Casal, H. L., and R. N. McElhaney. 1990. Quantitative determination of hydrocarbon chain conformational order in bilayers of saturated phosphatidylcholine of various chain lengths by Fourier transform infrared spectroscopy. *Biochemistry.* 29:5423–5427.
38. Fringeli, U. P. 1977. The structure of lipids and proteins studied by attenuated total reflection (ATR) infrared spectroscopy. II. Oriented layers of a homologous series: phosphatidylethanolamine to phosphatidylcholine. *Z. Naturforsch.* 32c:20–45.
39. Brandenburg, K., and U. Seydel. 1991. Correlations between FT-

IR spectroscopic and X-ray small-angle diffraction data and non-lamellar structures of lipopolysaccharides. *In* Spectroscopy of Biological Molecules. R. E. Hester and R. B. Girling, editors. Bookcraft, Bath, UK. 191–192.

40. Lindblom, G., and L. Rilfors. 1989. Cubic phases and isotropic structures formed by membrane lipids—possible biological relevance. *Biochim. Biophys. Acta.* 988:221–256.
41. Mariani, P., V. Luzzati, and H. Delacroix. 1988. Cubic phases of lipid-containing systems. Structure analysis and biological implications. *J. Mol. Biol.* 204:165–189.
42. Seddon, J. M. 1990. Structure of the inverted hexagonal (H_{II}) phase, and non-lamellar phase transitions of lipids. *Biochim. Biophys. Acta.* 1031:1–69.
43. Tate, M. W., E. F. Eikenberry, D. C. Turner, E. Shyamsunder, and S. M. Gruner. 1991. Nonbilayer phases of membrane lipids. *Chem. Phys. Lipids.* 57:147–164.
44. Green, P. M., J. T. Mason, T. J. O'Leary, and I. W. Levin. 1987. Effects of hydration, cholesterol, amphotericin B, and cyclosporin A on the lipid bilayer interface region: an infrared spectroscopic study using 2-[1-^{13}C] dipalmitoylphosphatidylcholine. *J. Phys. Chem.* 91:5099–5103.
45. Bush, S. F., Levin, H., and I. W. Levin. 1980. Cholesterol-lipid interactions: an infrared and Raman spectroscopic study of the carbonyl stretching mode region of 1,2-dipalmitoyl phosphatidylcholine bilayers. *Chem. Phys. Lipids.* 27:101–111.
46. Mushayakarara, E., and I. W. Levin. 1982. Determination of acyl chain conformation at the lipid interface region: Raman spectroscopic study of the carbonyl stretching mode region of dipalmitoyl phosphatidylcholine and structurally related molecules. *J. Phys. Chem.* 86:2324–2327.
47. Lotta, T. I., I. S. Salonen, J. A. Virtanen, K. K. Eklund, and P. K. Kinnunen. 1988. Fourier transform infrared study of fully hydrated dimyristoylphosphatidylglycerol. Effects of Na^+ on the *sn*-1′ and *sn*-3′ headgroup stereoisomers. *Biochemistry.* 27:8158–8169.
48. Mushayakarara, E., N. Albon, and I. W. Levin. 1982. Effect of water on the molecular structure of a phosphatidylcholine hydrate. Raman spectroscopic analysis of the phosphate, carbonyl and carbon-hydrogen stretching mode regions of 1,2-dipalmityol phosphatidylcholine hydrate. *Biochim. Biophys. Acta.* 686:153–159.
49. Casal, H. L., H. H. Mantsch, and H. Hauser. 1989. Infrared and ^{31}P-NMR studies of the interaction of Mg^{2+} with phosphatidylserines: effect of hydrocarbon chain unsaturation. *Biochim. Biophys. Acta.* 982:228–236.
50. Laroche, G., E. J. Dufourc, J. Dufourq, and M. Pézolet. 1991. Structure and dynamics of dimyristoylphosphatidic acid/calcium complexes by ^{2}H NMR, infrared, and Raman spectroscopic and small-angle X-ray diffraction. *Biochemistry.* 30:3105–3114.
51. Dluhy, R. A., D. G. Cameron, H. H. Mantsch, and R. Mendelsohn. 1983. Fourier transform infrared spectroscopic studies of the effect of calcium ions on phosphatidylserine. *Biochemistry.* 22:6318–6325.
52. Amey, R. L., and D. Chapman. 1984. Infrared spectroscopic studies of model and natural biomembranes. *In* Biomembrane Structure and Function. D. Chapman, editor. Verlag Chemie, Weinheim. 199–256.
53. Mendelsohn, R., M. A. Davies, J. W. Brauner, H. F. Schuster, and R. A. Dluhy. 1989. Quantitative determination of conformational disorder in the acyl chains of phospholipid bilayers by infrared spectroscopy. *Biochemistry.* 28:8934–8939.
54. Coughlin, R. T., A. Haug, and E. J. McGroarty. 1983. Physical properties of defined lipopolysaccharide salts. *Biochemistry.* 22:2007–2013.
55. Arrondo, J. L. R., F. M. Goni, and J. M. Macarulla. 1984. Infrared spectroscopy of phosphatidylcholine in aqueous suspensions. A study of the phosphate group vibrations. *Biochim. Biophys. Acta.* 794:165–168.
56. Goni, F. M., and J. L. R. Arrondo. 1986. A study of phospholipid phosphate groups in model membranes by Fourier transform infrared spectroscopy. *Faraday Discuss. Chem. Soc.* 81:117–126.
57. Cheng, K. H. 1991. Infrared study of the polymorphic phase behaviour of dioleoylphosphatidylethanolamine and dioleoylphosphatidylcholine mixtures. *Chem. Phys. Lipids.* 60:119–125.
58. Brade, L., K. Brandenburg, H.-M. Kuhn, S. Kusumoto, I. Macher, E. Th. Rietschel, and H. Brade. 1987. The immunogenicity and antigenicity of lipid A are influenced by its physicochemical state and environment. *Infect. Immun.* 55:2636–2644.